Supplementary Information

Absorbed hydrogen enhances the catalytic hydrogenation activity of Rh-based nanocatalysts

Franck Morfin[1], Lucie Blondeau[2], Karine Provost[2], Abdelmalek Malouche[2], Laurent Piccolo[1] and Claudia Zlotea[2*]*

[1] Univ Lyon, Université Claude Bernard - Lyon 1, CNRS, IRCELYON - UMR 5256, 2 Avenue Albert Einstein, F-69626 VILLEURBANNE CEDEX, France

[2] Université Paris Est, Institut de Chimie et des Matériaux Paris-Est (UMR 7182), CNRS, UPEC, 2-8 rue Henri Dunant, F-94320 Thiais, France

Figure S1. XRD patterns of carbon support (HSAG) and RhH_x@HSAG.

Figure S2. Conversion of butadiene and selectivity into butenes on Rh and RhH_x catalysts as a function of time on stream at 22°C for various gas feeds.

Figure S3. Ratio of the conversions of butadiene on Rh and RhH_x catalysts as a function of time on stream at 22°C for various gas feeds. In order to reflect reliable activity amplifications, the data points corresponding to more than 75% conversion of butadiene for Rh and/or RhH_x are not plotted.

Figure S4. Conversion and the selectivity into butenes as a function of temperature for Rh and RhH_x catalysts in a feed mixture C_4H_6:H_2 = 2:10%.

Figure S5. (a) Relationship between selectivity into butenes and butadiene conversion for Rh and RhH_x catalysts various reactant mixtures. (b) Zoom on the low-conversion area. It should be noted that the *cis*-2-butene impurity present in the gas feed with butadiene (0.3% of the total hydrocarbon amount) has been subtracted for the calculation of this distribution.

Figure S6. Distribution of the isomers of butene as function of conversion for the hydrogenation of 1,3 butadiene on Rh and RhH_x catalysts for two gas feed compositions.

Figure S7. XAS spectra of Rh nanoparticles under H_2 and reaction quasi-stationary conditions in hydride and metallic states. The XANES region is also shown in the inset. For comparison, the spectrum of bulk Rh is also plotted.

Figure S8. EXAFS spectra and corresponding FT of metal Rh nanoparticles during the hydrogenation of butadiene under 0.5% C_4H_6 and 2.5% H_2 in He (36 ml min^{-1}).

Figure S9. EXAFS spectra and corresponding FT of hydride RhH_x nanoparticles during the hydrogenation of butadiene under 0.5% C_4H_6 and 2.5% H_2 in He (36 ml min^{-1}).

Figure S10. *Operando* EXAFS-MS experiment for hydrogenation of butadiene (C_4H_6:H_2 = 0.5:2.5% in He, 1 atm, 36 ml/min, RT) on C-supported Rh and RhH_x catalysts. Hydrocarbon contents derived from smoothed MS intensities with m/z = 39, 41, and 43, accounting for (i) the relative fragment peak intensities for the pure compounds (1,3-butadiene, 1-butene and butane) and (ii) the total fragment distribution.

Figure S1. XRD patterns of carbon support (HSAG) and RhH_x@HSAG.

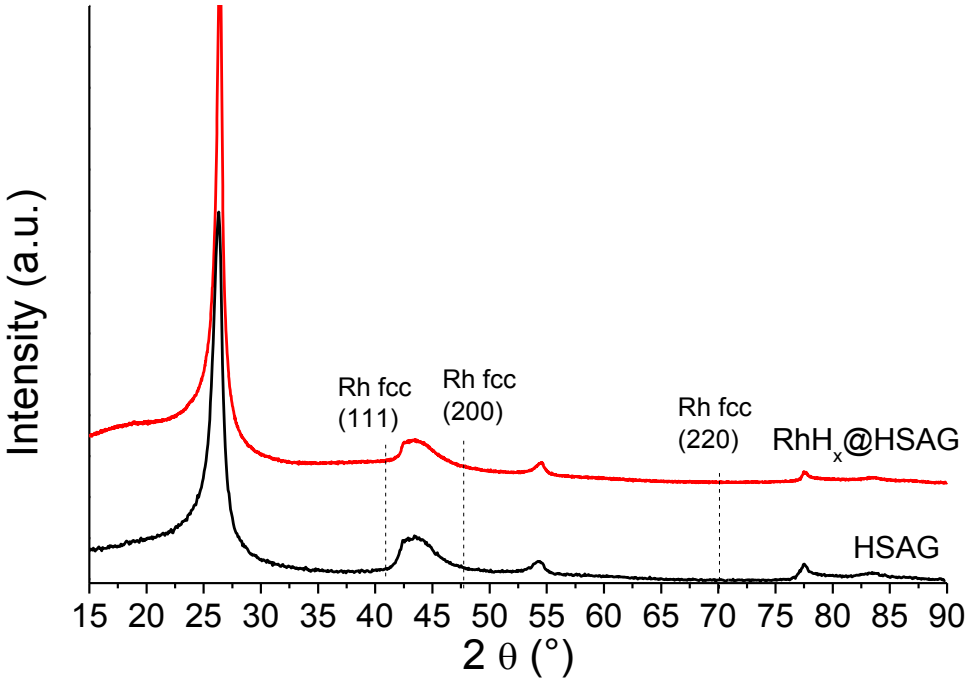

Figure S2. Conversion of butadiene and selectivity into butenes on Rh and RhH_x catalysts as a function of time on stream at 22°C for various gas feeds.

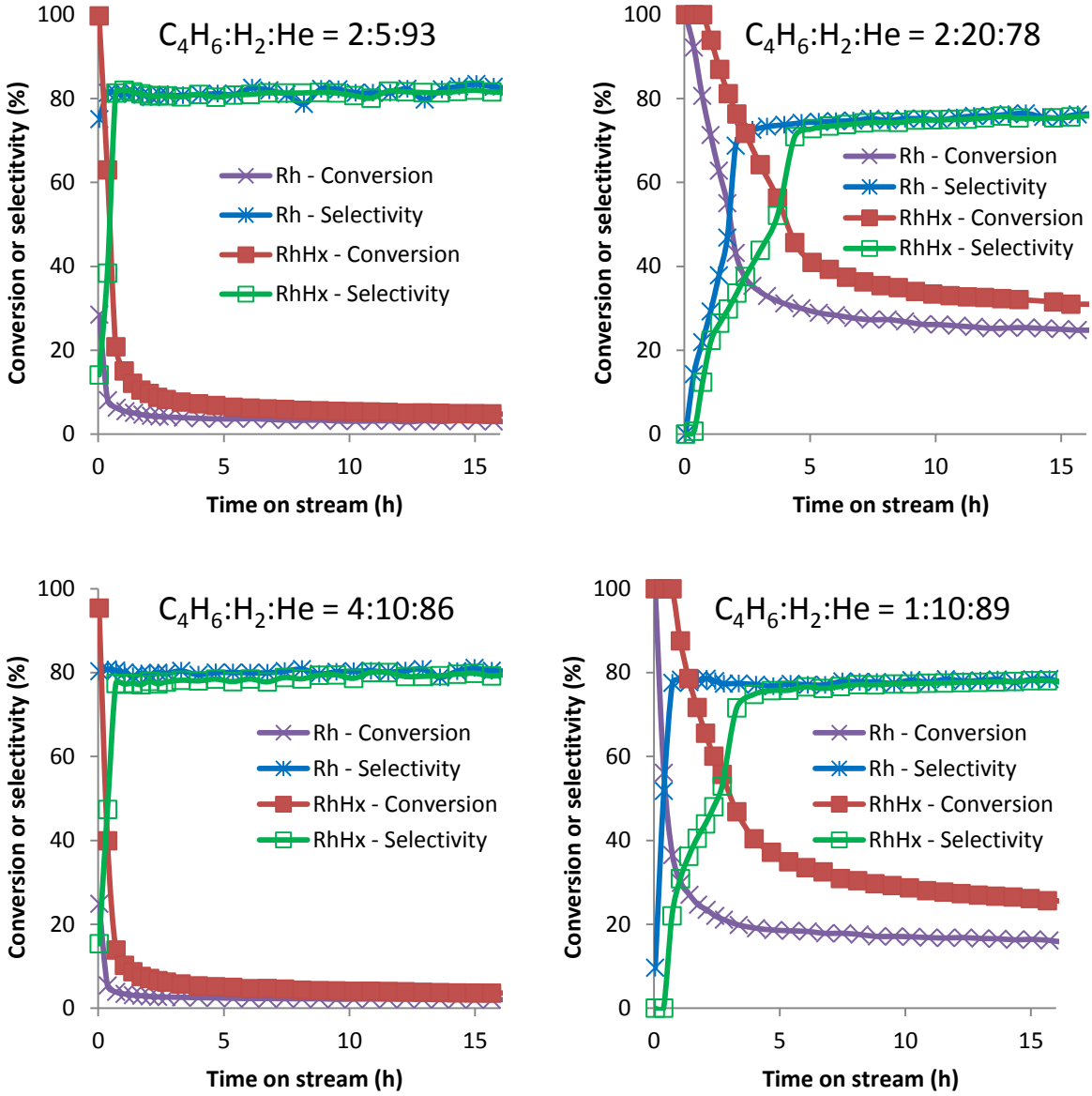

Figure S3. Ratio of the conversions of butadiene on Rh and RhH_x catalysts as a function of time on stream at 22°C for various gas feeds. In order to reflect reliable activity amplifications, the data points corresponding to more than 75% conversion of butadiene for Rh and/or RhH_x are not plotted.

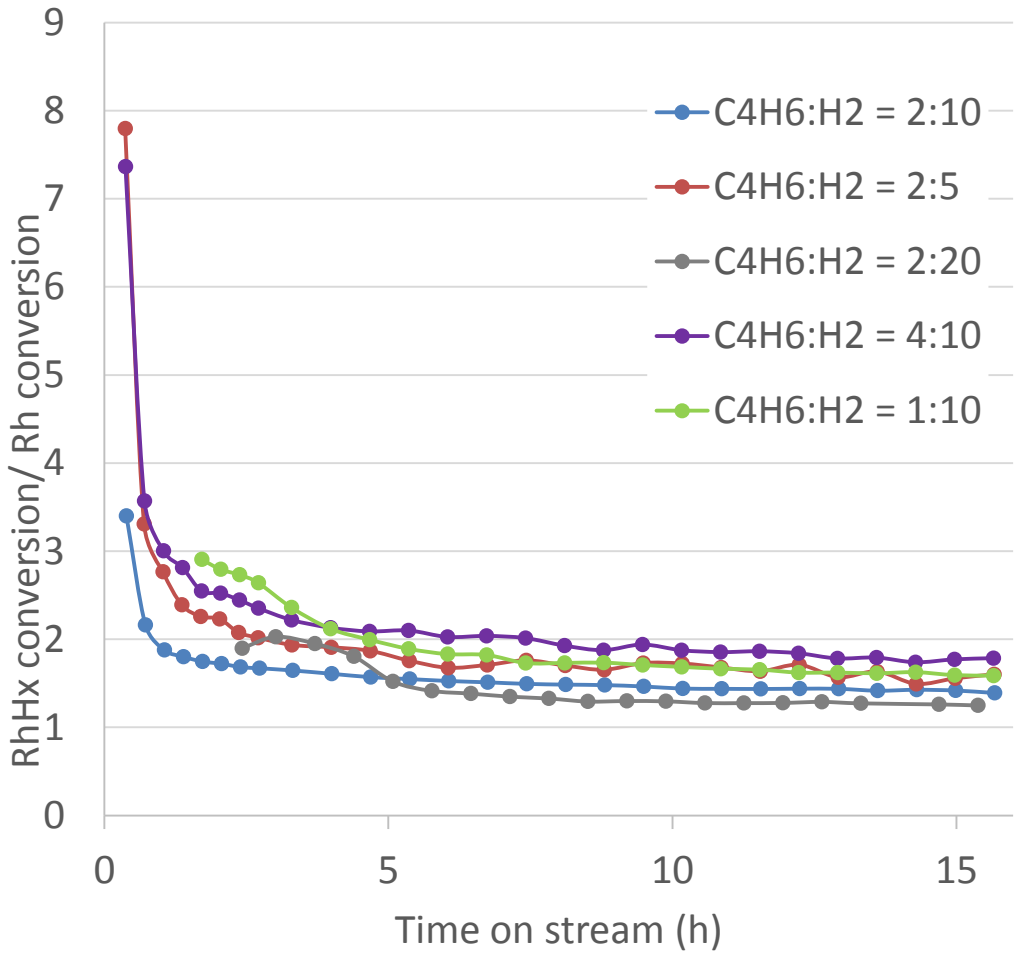

Figure S4. Conversion and the selectivity into butenes as a function of temperature for Rh and RhH_x catalysts in a feed mixture C_4H_6:H_2 = 2:10%.

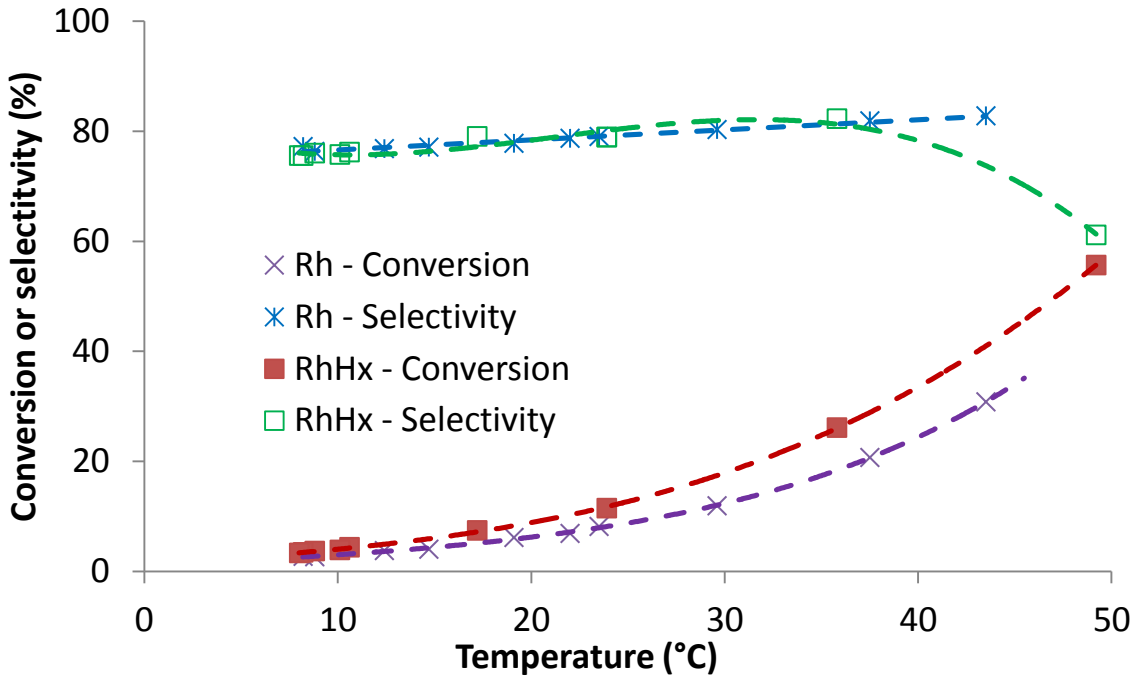

Figure S5. (a) Relationship between selectivity into butenes and butadiene conversion for Rh and RhH_x catalysts various reactant mixtures. (b) Zoom on the low-conversion area. It should be noted that the *cis*-2-butene impurity present in the gas feed with butadiene (0.3% of the total hydrocarbon amount) has been subtracted for the calculation of this distribution.

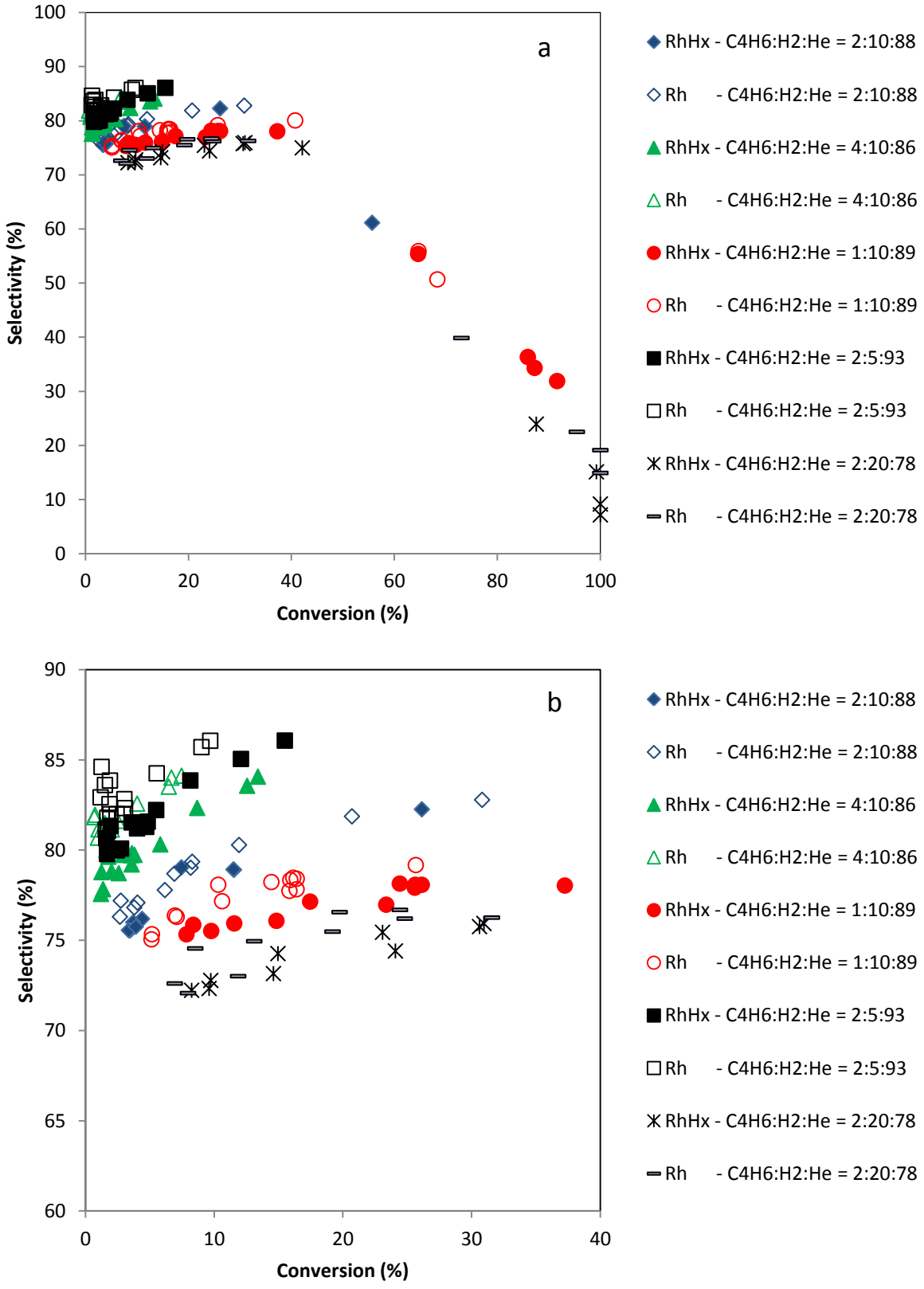

Figure S6. Distribution of the isomers of butene as function of conversion for the hydrogenation of 1,3 butadiene on Rh and RhH_x catalysts for two gas feed compositions.

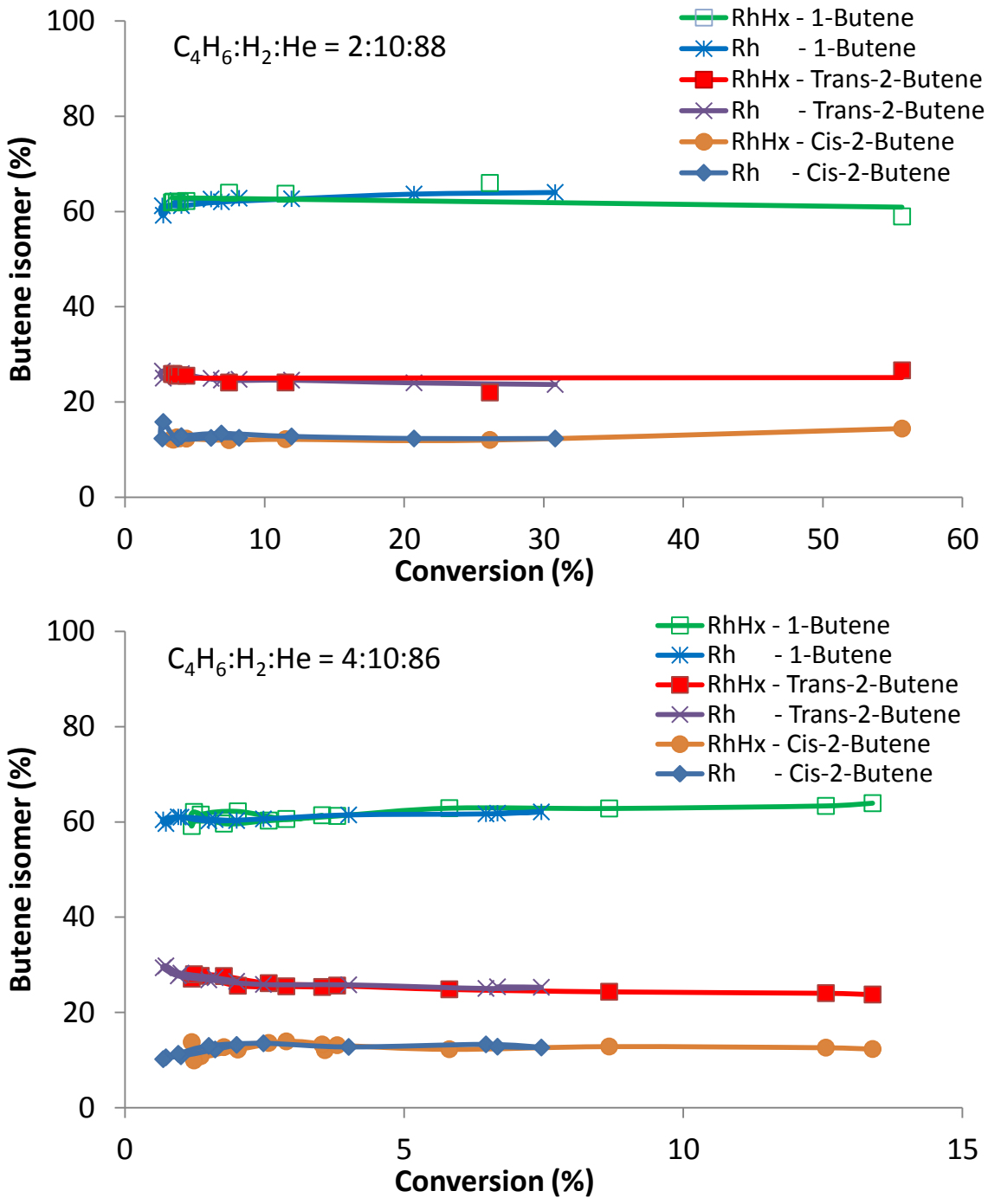

Figure S7. XAS spectra of Rh nanoparticles under H_2 and reaction quasi-stationary conditions in hydride and metallic states. The XANES region is also shown in the inset. For comparison, the spectrum of bulk Rh is also plotted.

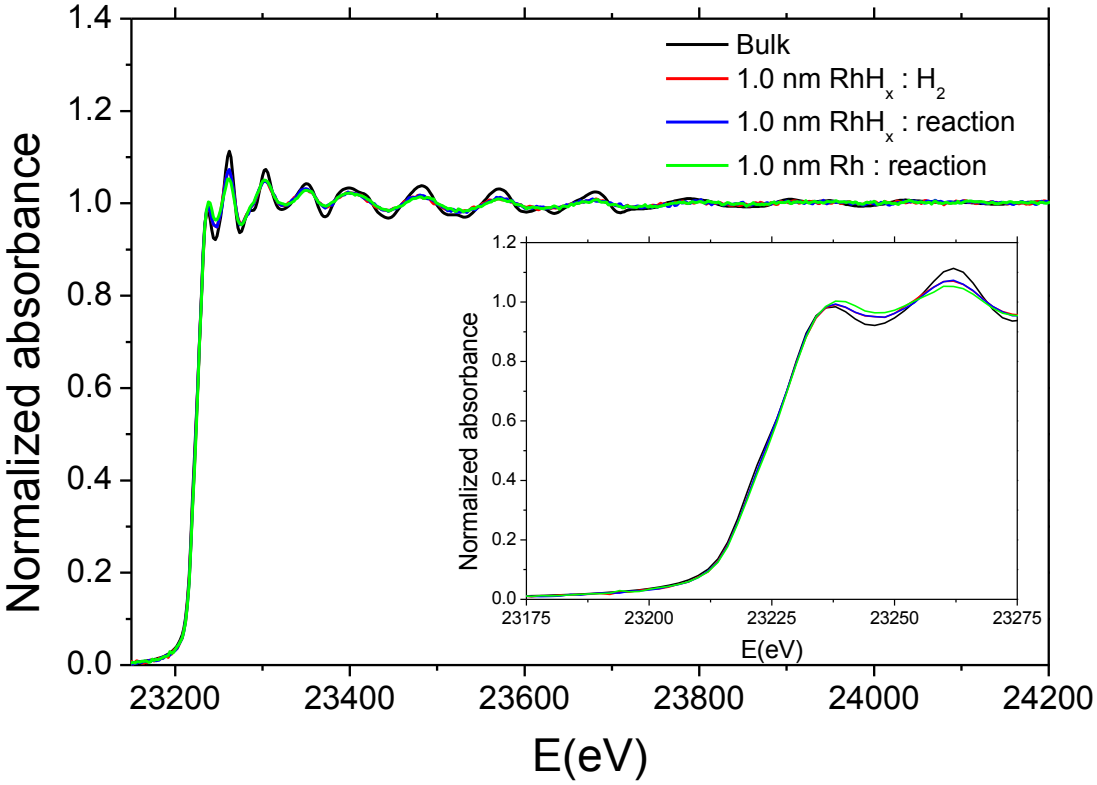

Figure S8. EXAFS spectra and corresponding FT of metal Rh nanoparticles during the hydrogenation of butadiene under 0.5% C_4H_6 and 2.5% H_2 in He (36 ml min^{-1}).

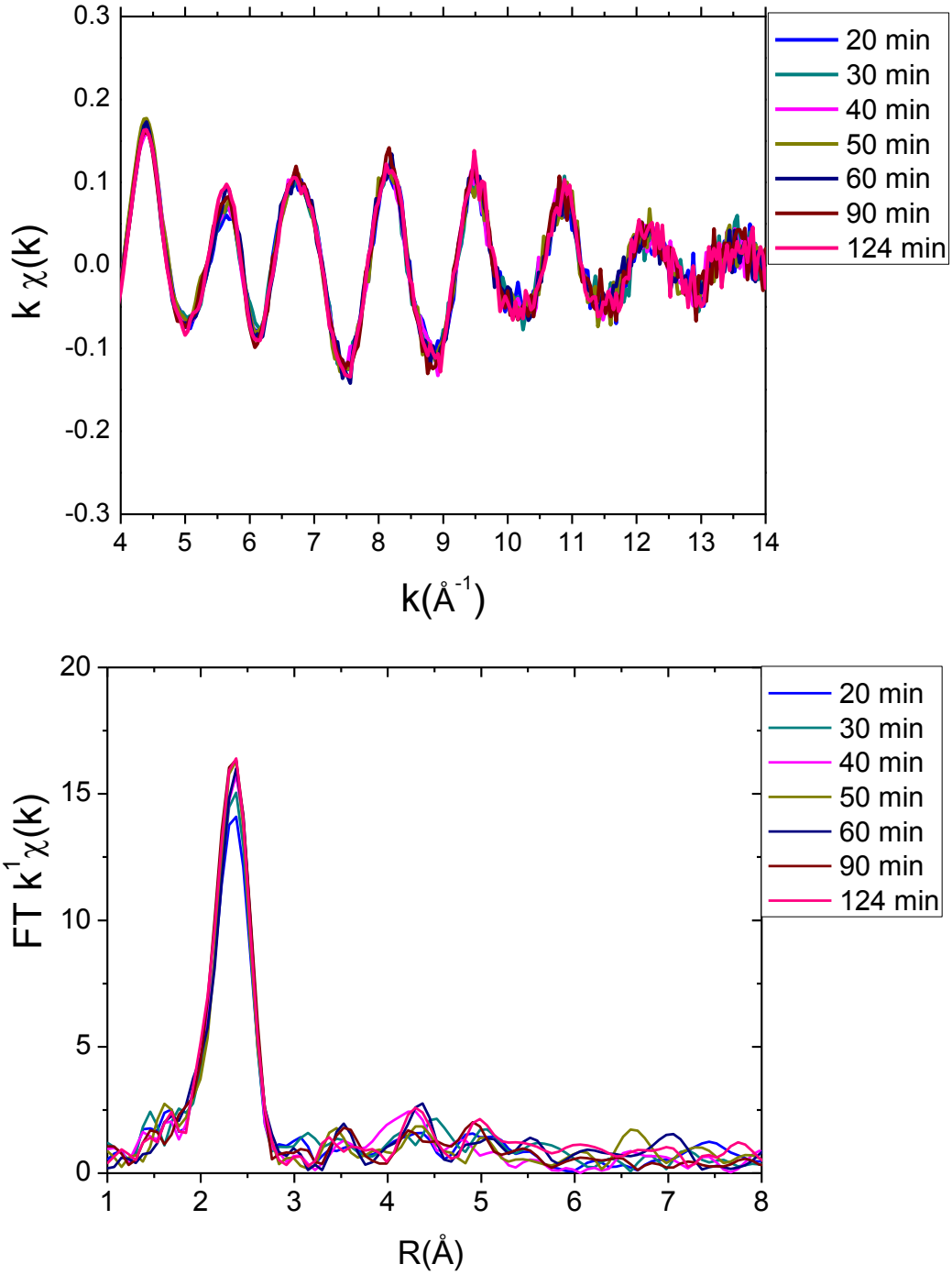

Figure S9. EXAFS spectra and corresponding FT of hydride RhH_x nanoparticles during the hydrogenation of butadiene under 0.5% C_4H_6 and 2.5% H_2 in He (36 ml min^{-1}).

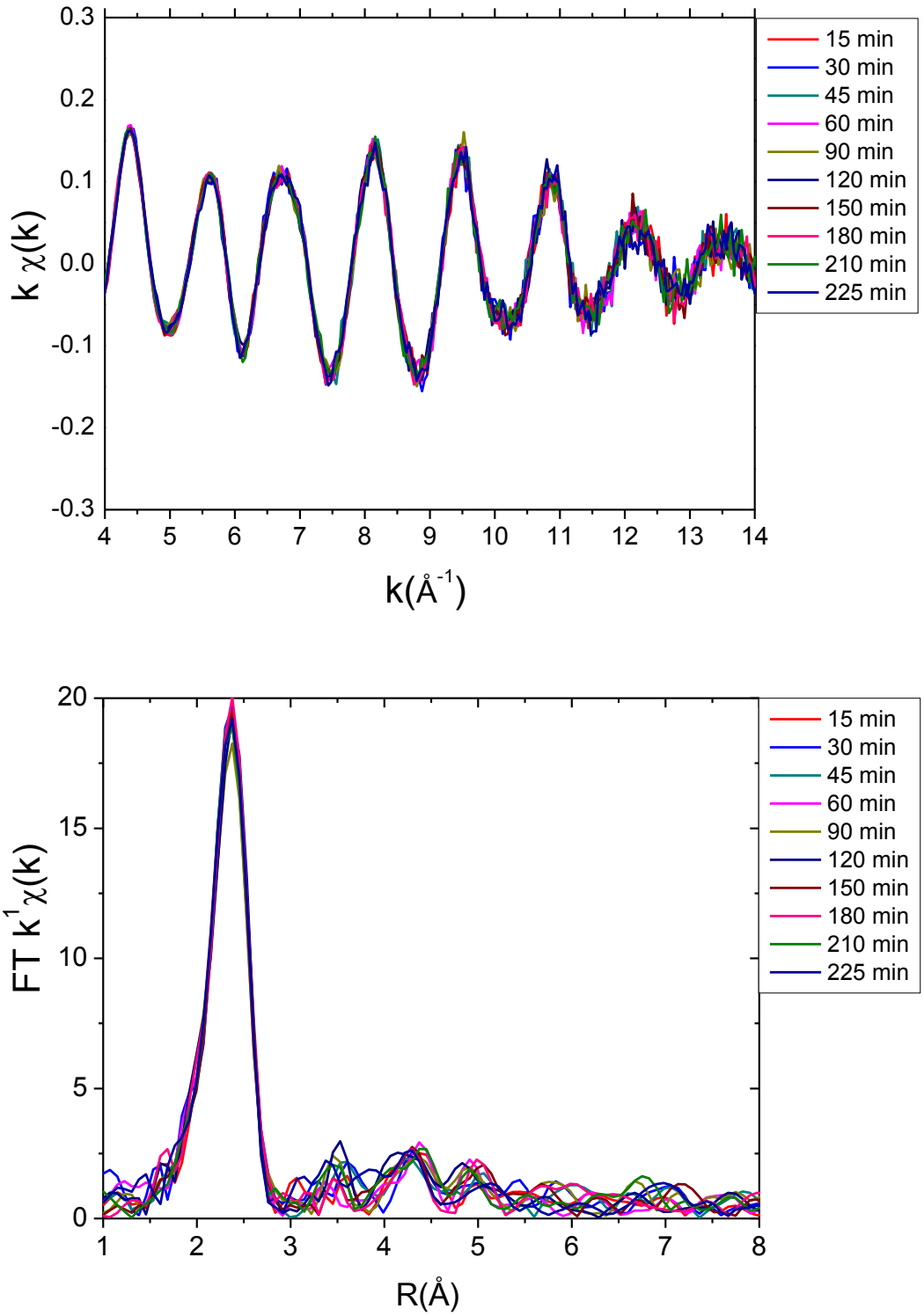

Figure S10. *Operando* EXAFS-MS experiment for hydrogenation of butadiene (C_4H_6:H_2 = 0.5:2.5% in He, 1 bar, 36 ml min^{-1}, RT) on C-supported Rh and RhH_x catalysts. Hydrocarbon contents derived from smoothed MS intensities with m/z = 39, 41, and 43, accounting for (i) the relative fragment peak intensities for the pure compounds (1,3-butadiene, 1-butene and butane) and (ii) the total fragment distribution.